

# Predicting electrical and thermal abuse behaviours of practical lithium-ion cells from accelerating rate calorimeter studies on small samples in electrolyte

M.N. Richard, J.R. Dahn \*

*Department of Physics, Dalhousie University, Halifax, Nova Scotia, Canada, B3H 3J5*

Received 14 October 1998; accepted 22 December 1998

## Abstract

An accelerating rate calorimeter (ARC) is used to measure the thermal stability of de-intercalated  $\text{Li}_{1+x}\text{Mn}_{2-x}\text{O}_4$  in  $\text{LiPF}_6$  EC:DEC (33:67) electrolyte. Self-heating is detected well after the  $80^\circ\text{C}$  onset of self-heating measured for lithium intercalated mesocarbon microbead (MCMB) electrodes in  $\text{LiPF}_6$  EC:DEC (33:67) electrolyte. As a result, the initial self-heating measured in a practical carbon/ $\text{Li}_{1+x}\text{Mn}_{2-x}\text{O}_4$  lithium-ion cell is caused by reactions at the anode. In previous work, we have proposed a model for the reactions that cause self-heating in MCMB electrodes in electrolyte. By assuming that a cell self-heats only because reactions occur at the anode, the model can be used to predict the power generated by the amount of MCMB in practical cells with an inert cathode. The calculated chemically generated power can be combined with power loss measurements, due to the transfer of heat to the environment, to predict the short-circuit behaviour and the oven exposure behaviour for a cell containing an MCMB anode and an inert cathode. The results agree qualitatively with short-circuit and oven exposure results measured on NEC Moli energy 18650 cells containing an  $\text{Li}_{1+x}\text{Mn}_{2-x}\text{O}_4$  cathode. © 1999 Elsevier Science S.A. All rights reserved.

**Keywords:** Lithium-ion cells; Accelerating rate calorimeter; Electrolyte

## 1. Introduction

Industry typically uses tests described in Underwriters' Laboratories 1642 [1] to simulate different abuse conditions in a lithium-ion cell. These tests give qualitative information concerning the thermal stability of an entire battery, but they do not give any information concerning the reactions that produce heat at each electrode or on the parameters that affect the volatility of the electrodes.

Our goal is to devise a method to test the reactivity, at elevated temperatures, of a small amount of electrode material in electrolyte. Once the mechanisms generating heat are known, materials science solutions, such as coatings or additives to the electrolyte, can be used to lessen the reaction rate. Knowledge of the mechanism(s) generating heat will explain why these strategies enhance thermal stability or make it possible to propose new strategies to improve thermal stability. With this knowledge of the

reaction mechanism(s), quantitative predictions concerning the behaviour of practical lithium-ion cells subjected to thermal or electrical abuse can be made.

Using an accelerating rate calorimeter (ARC), we studied an MCMB electrode in electrolyte in order to understand the effects of initial heating temperature, lithium content, binder and electrolyte type on the self-heating rate. These results allowed us to propose a mechanism for the processes that generate heat when lithiated MCMB is placed in electrolyte and heated to elevated temperature [2].

In this paper, some preliminary ARC results collected on  $\text{Li}_{1+x}\text{Mn}_{2-x}\text{O}_4$  in  $\text{LiPF}_6$  EC:DEC (33:67) electrolyte are presented. These results are combined with the previously reported results for MCMB in  $\text{LiPF}_6$  EC:DEC (33:67) to predict: (1) the necessary shutdown temperature for a separator in a cell containing these electrodes; (2) the  $60^\circ\text{C}$  short-circuit behaviour of an 18650 lithium-ion cell containing these electrodes; and (3) the  $150^\circ\text{C}$  oven exposure behaviour of an 18650 cell containing an MCMB anode and a cathode which is inert to  $150^\circ\text{C}$ .

\* Corresponding author. Tel.: +1-902-494-2312; E-mail: jeff.dahn@dal.ca

## 2. Experimental

$\text{Li}_{1+x}\text{Mn}_{2-x}\text{O}_4$  (Chemetals T202), which has a surface area of  $1.7 \text{ m}^2/\text{g}$  and  $x$  about equal to 0.05, was de-lithiated electrochemically. Electrodes were made by combining: 7% by mass of Super S Carbon Black (MMM), 7% by mass of polyvinylidene difluoride (PVDF) binder and  $\text{Li}_{1+x}\text{Mn}_{2-x}\text{O}_4$  active material in a nalgene bottle containing zirconia media beads Extra 1-methyl pyrrolidinone (NMP) is added to make the mixture less viscous. This mixture is shaken for approximately 10 min and then poured into a stainless steel boat and dried at  $110^\circ\text{C}$  for a minimum of 3 h. The resulting powder is passed through a  $300 \mu\text{m}$  stainless steel mesh. About 490 mg of the sieved powder is then poured into a stainless steel pellet press and 3000 psi applied to make a 1 mm thick electrode pellet. The electrode is brought into an argon-filled glove box where coin cell construction proceeds.

Cell construction proceeds as shown in Fig. 1. The pellet is placed in the bottom of a 2325 coin cell.  $\text{LiPF}_6$  EC:DEC (33:67) electrolyte is added until the surface of the pellet remains wet. Two polypropylene 2502 separators are placed above the pellet. A stainless steel mesh is added above the separator. The lithium removed from the cathode on charge will plate onto this mesh, hence it also acts as the reference electrode in the cell. Two stainless steel spacers are placed above the stainless steel mesh. A polypropylene gasket is pressed onto the cell top. The top is added above the spacer, and the cell is placed into a crimper where the edges of the cell can be folded over the top of the can. Stainless steel tabs are spot-welded onto the cell can.

A signature curve charge test is used to de-lithiate the  $\text{Li}_{1+x}\text{Mn}_{2-x}\text{O}_4$  cathodes. Initially, the controller was set to a 4 mA current to remove lithium quickly. Once the cell

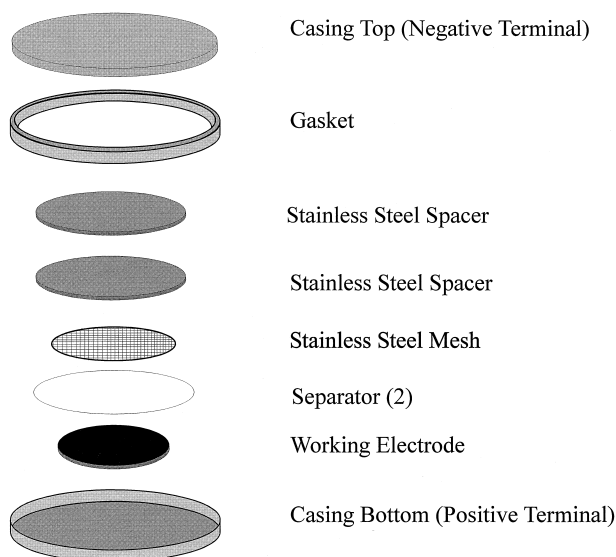


Fig. 1. Exploded view of pellet coin cell.

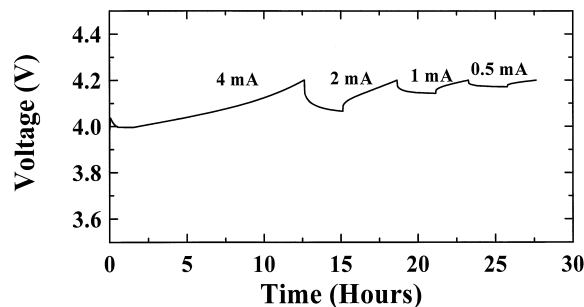


Fig. 2. Signature curve charge profile for  $\text{LiMn}_2\text{O}_4$  (Chemetals, T202) charged to 4.3 V in  $\text{LiPF}_6$  EC:DEC (33:67). The initial current was 4 mA.

potential reached the voltage set point, the current stopped and the cell relaxed for 2.5 h. The cell was charged three more times but the current was reduced by 50% on each subsequent cycle. The result is a cell that equilibrates at the chosen potential. A typical example of this test is shown in Fig. 2. The cells were charged to 4.3 V in order to remove almost all the lithium. Once the cell had equilibrated at the set potential, it was removed from the charger and brought into an argon-filled glove box for ARC sample construction. ARC sample construction is described elsewhere [2].

## 3. Results and discussion

ARC results for samples containing only electrolyte, presented in [2], showed that self-heating, which began at approximately  $190^\circ\text{C}$ , was preceded by a temperature decrease caused by an endothermic reaction. ARC results for fresh MCMB in electrolyte were also presented there and showed that fresh MCMB in electrolyte is inert. The ARC results for fresh  $\text{Li}_{1+x}\text{Mn}_{2-x}\text{O}_4$  (T202) in  $\text{LiPF}_6$  EC:DEC (33:67) electrolyte are shown in Fig. 3. There is a small amount of self-heating initially detected at  $130^\circ\text{C}$ . X-ray diffraction measurements made on the powder retrieved after the experiment showed that the lattice constant was  $8.168 \text{ \AA}$ . The lattice constant for the original powder was  $8.2155 \text{ \AA}$ . The lattice is smaller after the ARC experiment. In situ X-ray diffraction experiments on  $\text{Li}_{1+x}\text{Mn}_{2-x}\text{O}_4$  have shown that the lattice constant decreases as  $\text{Mn}^{3+} \rightarrow \text{Mn}^{4+}$  [3]. In the fresh  $\text{Li}_{1+x}\text{Mn}_{2-x}\text{O}_4$  ARC sample, this transition could occur if manganese dissolved in the electrolyte, a phenomenon reported by Tarascon et al. [4]. The self-heating rate is low, barely above the detection limit of the ARC; hence, this is not a significant reaction as long as the surface area of the material remains relatively low.

The self-heating rate profile for  $\text{Li}_{1+x}\text{Mn}_{2-x}\text{O}_4$  charged to 4.3 V (115 mAh/g) is shown in Fig. 4. Self-heating is detected at approximately  $140^\circ\text{C}$ . The profile has many features, which indicates that there are many processes generating heat in this spinel material. This has been reported before by Reimers et al. [5]. The nature of all the

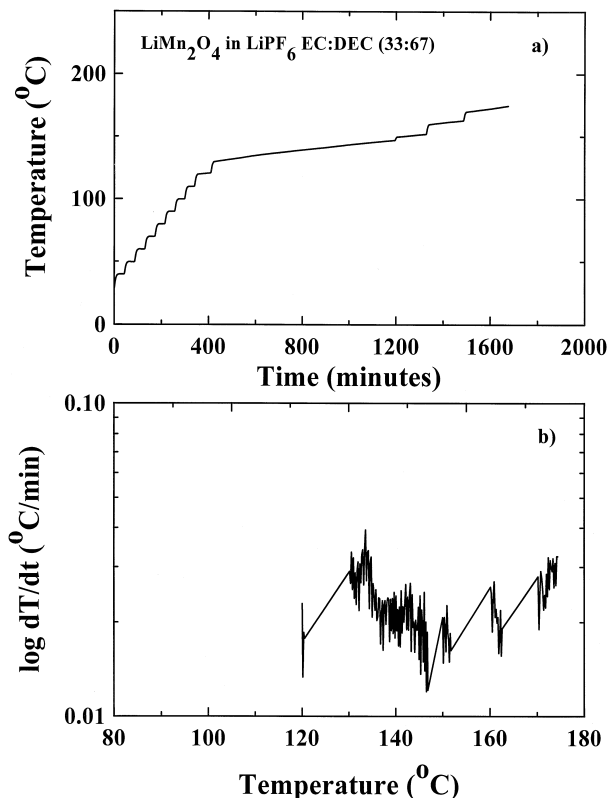


Fig. 3. Self-heating rate profiles for fresh  $\text{LiMn}_2\text{O}_4$  in  $\text{LiPF}_6$  EC:DEC (33:67) Electrolyte: (a) the temperature vs. time profile and (b) the self-heating rate profile.

processes is as yet unknown. By comparison to the results in Fig. 3 for fresh spinel, the reaction between the electrolyte and delithiated spinel is much faster and more exothermic as expected.

ARC results from MCMB electrodes, containing PVDF binder, in  $\text{LiPF}_6$  EC:DEC (33:67) electrolyte have already been reported [2]. The results showed that MCMB samples containing PVDF and discharged in  $\text{LiPF}_6$  EC:DEC (33:67) had a detectable exotherm starting at  $80^\circ\text{C}$  and had two features: (1) a peak, which was attributed to the decompo-

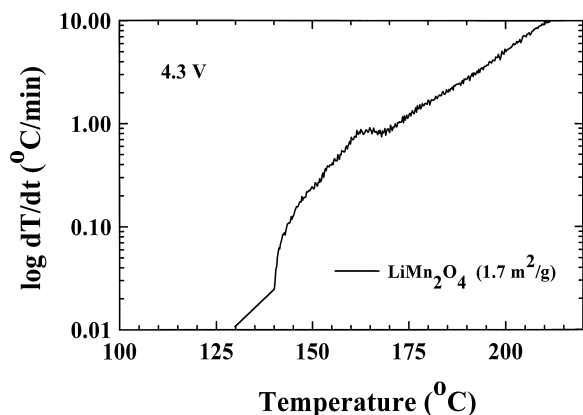


Fig. 4. Self-heating rate profile for  $\text{LiMn}_2\text{O}_4$  (Chemetals) charged to 4.3 V in  $\text{LiPF}_6$  EC:DEC (33:67) electrolyte.

sition of the metastable components of the SEI; and (2) a tail, attributed to the formation of new SEI. If the MCMB samples are heated to a higher initial temperature, the self-heating rate increases. These trends are all shown in the results presented in Fig. 5. Also in Fig. 5 is the ‘universal’ line which fits through the initial slope of any self-heating rate profile of lithiated MCMB in  $\text{LiPF}_6$  EC:DEC (33:67). This ‘universal’ line was used to determine the activation energy ( $E$ ) and the frequency factor ( $A$ ) for the conversion of metastable SEI components to stable SEI components.

Independent of the processes that generate heat in the  $\text{Li}_{1+x}\text{Mn}_{2-x}\text{O}_4$  and the MCMB samples, it is interesting and useful that self-heating in  $\text{Li}_{1+x}\text{Mn}_{2-x}\text{O}_4$  samples is only detected at higher temperatures compared to the behaviour of the MCMB electrode. As a first approximation, the behaviour of practical cells during thermal or electrical abuse can be predicted by assuming the cathode is inert and any initial self-heating in the cell is due to the reactions that occur at the MCMB electrode.

The ARC measures the temperature of a sample as it self-heats. For each temperature measurement, it measures the corresponding time. As a result, the self-heating of the sample (in  $^\circ\text{C}/\text{min}$ ) can be calculated. The self-heating of the ARC samples can be used to calculate the power generated by the reaction(s). The relation to calculate power is:

$$P = Cm \frac{dT}{dt} \quad (1)$$

where  $C$  is the specific heat of the entire sample (material + electrolyte + sample holder) and  $m$  is the mass of the entire sample.

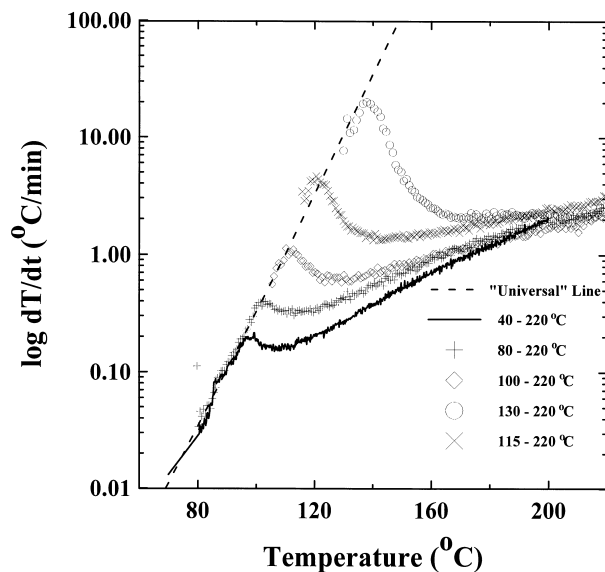


Fig. 5. ‘Universal’ line through the initial slope of the self-heating rate profiles collected on samples containing lithiated MCMB in  $\text{LiPF}_6$  EC:DEC (33:67) heated to different initial temperatures ( $80^\circ\text{C}$ ,  $100^\circ\text{C}$ ,  $115^\circ\text{C}$  and  $130^\circ\text{C}$ ).

When the specific heat and mass of the entire sample are used, Eq. (1) compensates for any heat used to increase the temperature of the sample holder. The specific heat,  $C$ , was obtained by summing the relative percent of the specific heats of each of the components of the sample. Typically, the stainless steel sample holder makes up 50% of the mass, the powder 20% and the electrolyte the remaining 30%. The specific heat for the MCMB samples is therefore approximately:

$$\begin{array}{l} \text{Stainless steel} \quad \text{Graphite} \quad \text{Electrolyte} \\ C = 0.5(0.46) + 0.2(0.71) + 0.30(1.53) = 0.83 \text{ J/(gK)} \end{array} \quad (2)$$

where the specific heat values of graphite, stainless steel, EC and DEC were found in *The Thermophysical Properties of Matter* [6]. The mass,  $m$ , of an ARC sample is about 1.8 g typically.

The calculated power curves for the MCMB material, initially heated to 80°C, 100°C, 115°C and 130°C, are shown in Fig. 6. The power is calculated by multiplying the self-heating rate measured in the ARC by constants ( $Cm$ ), hence the general shape of the power vs. temperature profiles is the same as the self-heating rate profiles presented in Fig. 5.

The power curves in Fig. 6 represent the total power generated by the ARC sample, hence they can be used to predict the power generated by the material in an 18650 cell. An 18650 cell contains approximately 5 g of MCMB and 5 g of electrolyte. The power generated in an 18650 cell is therefore:

$$P_{18650} = P_{\text{ARC}} \frac{m_{18650}}{m_{\text{ARC}}} \quad (3)$$

where  $m_{18650}$  is the mass of the electrode and electrolyte in an 18650 cell (10 g) and  $m_{\text{ARC}}$  is the mass of powder and electrolyte in the ARC sample (0.4 g wet powder and 0.4 g

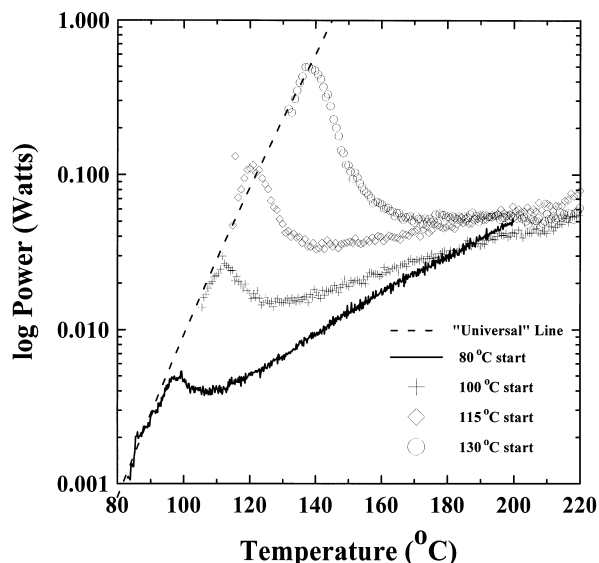


Fig. 6. The calculated power generated in an ARC sample, for MCMB discharged to 0.0 V in LiPF<sub>6</sub> EC:DEC (33:67).

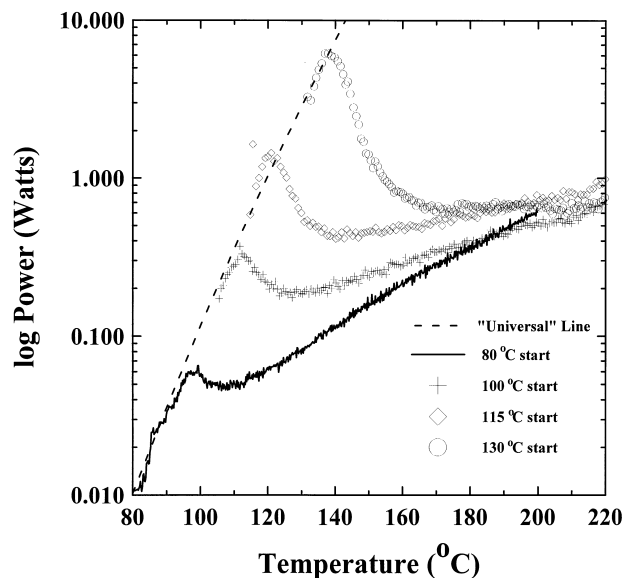


Fig. 7. The calculated power generated by the MCMB material in LiPF<sub>6</sub> EC:DEC (33:67) in an 18650 cell can.

electrolyte). The calculated 18650 power curves for MCMB initially heated to 80°C, 100°C, 115°C and 130°C are shown in Fig. 7.

The cell can radiates heat, as a result, a cell that self-heats is not adiabatic. In order to properly predict the behaviour of lithium-ion cells when they self-heat, it is necessary to determine the heat transfer properties for different size cans and for different geometries. To simulate the heat generated by the chemical reactions of the electrodes in electrolyte, a wire wound resistor, with a 10-W and 10-Ω rating, was placed in an empty cell can. The cell can was vertically attached to a thin-walled stainless steel post and placed in an oven. The current through the resistor was increased from 0 to 1 A in 0.1-A steps. After each step, the cell can temperature was allowed to equilibrate for a minimum of 30 min. Then the voltage across the resistor and the temperature at the surface of the cell can were measured. The power loss in the resistor, which causes the heat and hence causes the cell can temperature to increase, is calculated from  $P = IV$ . Heat transfer measurements for 18650 cell cans were made in an oven at room temperature and at 150°C. The results are shown in Fig. 8. The 18650 cell can heat transfer profile has the same shape at both environmental temperatures. A similar heat transfer measurement was made on a 26500 cell can held vertically in an oven. The profile, shown in Fig. 8, is almost identical to the 18650 heat transfer profiles.

The self-heating rate results presented in Figs. 4 and 5 show that if a cell self-heats it will initially be because the MCMB reacts. As a first approximation then, the 'universal' line for MCMB in LiPF<sub>6</sub> EC:DEC (33:67), shown in Fig. 5, can be used to predict if a cell will self-heat. Just as the self-heating rate profiles were converted to generated

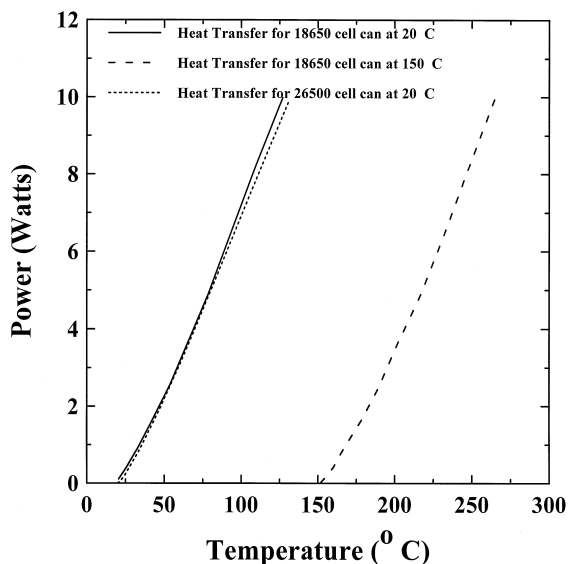


Fig. 8. Measured 18650 or 26500 cell can temperature when the power generated by a resistor is increased from 0 to 10 W.

power curves, so was the ‘universal’ line. When the ‘universal’ power line is compared to the power loss curve, the required shutdown temperature for the separator in a cell containing an MCMB anode and an inert cathode can be determined.

In a short-circuit test, the temperature of the lithium-ion cell rises from the environmental temperature to the separator shutdown temperature in about 1 min. Therefore, we assume that the lithiated MCMB and electrolyte in the cell are instantly ‘stepped’ to that temperature and use the ‘universal’ power curve to estimate how much chemically generated power is initially produced. If the chemically generated power is greater than that which the cell can will radiate, conduct or convect away, the cell will self-heat. If not, the cell will cool.

Fig. 9 shows the ‘universal’ power curve and the power loss curve for 20°C and 60°C ambient temperatures. Using the 20°C ambient power loss curve, we can predict that an 18650 Carbon/LiMn<sub>2</sub>O<sub>4</sub> lithium-ion cell will not self-heat unless the core temperature increases beyond about 143°C in a short circuit test from 20°C ambient. Similarly, a cell in a 60°C environment will not self-heat in a short-circuit test unless the core temperature increases beyond 138°C. ARC results are used to predict the behaviour of a 26500 cell. A mass of about 8.5 g of MCMB and about 8.5 g of electrolyte can be accommodated in a 26500 cell. From the results in Fig. 9, a 26500 cell in a 20°C environment will not self-heat in a short-circuit test unless the core temperature exceeds 135°C. If the 26500 cell is at 60°C, it will not self-heat unless some sort of abuse causes the core temperature to increase to a temperature in excess of about 131°C.

The model for self-heating due to reactions at the MCMB electrode, described in Ref. [7], can be used to make semi-quantitative predictions about the short-circuit

and oven exposure behaviour of lithium-ion cells. For simplicity, we assume that the internal temperature of the cell is uniform. The actual temperature gradients in the cell could be incorporated into more sophisticated models.

The temperature of a short-circuited cell will only increase if the generated heat is greater than the heat lost. In a short-circuited cell, heat is initially generated by the electrical current in the cell ( $P = IV$ ). At elevated temperatures the chemical reactions at the electrodes also generate heat. At each point in the numerical calculation, the electrical power due to the short-circuit,  $P_{\text{elec}}$ , and the chemically generated power due to the reaction of the MCMB,  $P_{\text{chem}}$ , are added, but then the power loss to the environment,  $P_{\text{out}}$ , is subtracted. At each step in the calculation, the total power producing the temperature increase,  $P(T)$ , is:

$$P(T) = P_{\text{elec}} + P_{\text{chem}} - P_{\text{out}} \quad (4)$$

where

$$P_{\text{elec}} = I^2 R \quad (5)$$

and from Ref. [7];

$$P_{\text{chem}} = \left[ \frac{h_1}{C} A_1 e^{\frac{-E_1}{k_B T}} x_f^n + \frac{h_2}{C} A_2 e^{\frac{-E_2}{k_B T}} x_i e^{\frac{-z}{z_0}} \right] C m \quad (6)$$

where the first term calculates the heat produced by the conversion of metastable SEI to stable SEI and the second term is the heat produced by the reaction of lithium with solvent to eventually form new stable SEI. The heats of reaction for the formation of stable SEI from metastable SEI and for the formation of stable SEI from lithium and solvent reaction are represented by  $h_1$  and  $h_2$ , respectively.  $C$  is the specific heat of the cell and  $h/C$  is the

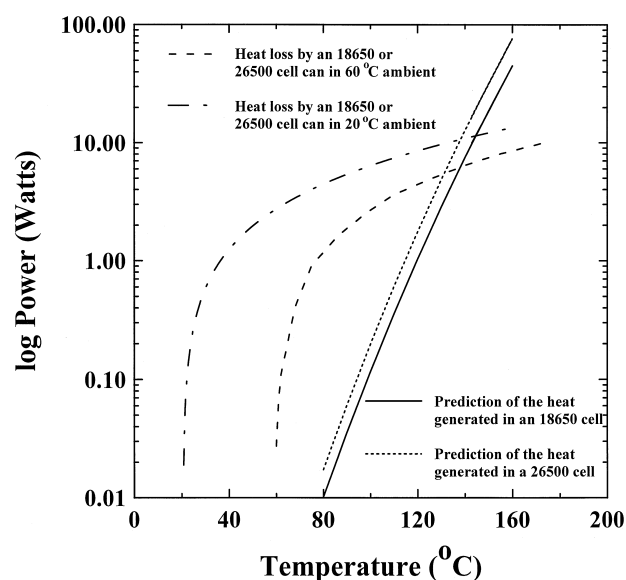


Fig. 9. Initial chemically generated power due to anode–electrolyte reactions in 18650 cells and 26500 cells and power loss curves for 18650 and 26500 cell cans in 20°C and 60°C ambient temperatures.

temperature increase caused by the heat produced in the reaction.  $E$  and  $A$  are the activation energy and the frequency factor for the different reactions. The amount of lithium intercalated into the carbon is represented by  $x_i$ , and the lithium in the metastable SEI is represented by  $x_f$ . The thickness of the SEI layer, is related to the amount of lithium present in both stable and metastable SEI components,  $z$ . The reaction order,  $n$ , is set to 0.5,  $k_B$  is Boltzmann's constant and  $T$  is the temperature of the cell. These factors and their values, which give good agreement with ARC experiments, are defined in greater detail in other work [7].  $P_{out}$  is the power vs. temperature curve from Fig. 8.

We assume that during short-circuit of an 18650 cell, an average current,  $I$ , is 25 A and the resistance,  $R$ , for the cell is about  $0.1 \Omega$  [8]. This current flows until the separator melts at  $130^\circ\text{C}$ . The temperature increase in the cell is:

$$dT = \frac{P(T)}{Cm} dt \quad (7)$$

where  $Cm$  is the heat capacity of the cell,  $45 \text{ J/K}$  [8]. The exact formula for  $P_{out}$  depends on the environmental temperature. A short-circuit test is usually measured at  $20^\circ\text{C}$  or at  $60^\circ\text{C}$  [1]. From Fig. 8, the power loss curves at each of these temperatures are:

$$P(20^\circ\text{C}) \text{ in Watts} = -1.06418 + 0.0468604T + 0.0002762T^2 \quad (T \text{ in } ^\circ\text{C}) \quad (8)$$

$$P(60^\circ\text{C}) \text{ in Watts} = -2.49666 + 0.0247636T + 0.00024621T^2 \quad (T \text{ in } ^\circ\text{C}) \quad (9)$$

The calculation, based on Eq. (4), will provide an estimate for the temperature at the core of the cell during a short-circuit experiment. The calculated and measured temperature vs. time profiles for a  $60^\circ\text{C}$  short-circuit experiment are shown in Fig. 10. The measured results were provided by NEC Moli Energy for an IMR18650 cell with a nominal capacity of 1.35 Ahr charged to 4.2 V. The results show that during a short-circuit experiment, the core temperature quickly increases to the melting temperature of the separator, which was set at  $130^\circ\text{C}$ . At this point, the electrical power stops because current can no longer flow. Panels c and d of Fig. 10 show that while current flows there is little change in the amount of lithium in the metastable SEI,  $x_f$ , or in the thickness of the SEI layer,  $z$ . However, due to the short-circuit, lithium moves from the anode to the cathode hence as we see in Fig. 10b, the amount of intercalated lithium,  $x_i$ , decreases during this period. The high core temperature causes the reactions at the anode to generate heat however this heat is insufficient to overcome cooling. The temperature of the cell containing MCMB and  $\text{LiPF}_6$  EC:DEC (33:67) will decrease to ambient temperature.

It is encouraging that the general shape of the short-circuit profile is correct. However, the results measured by

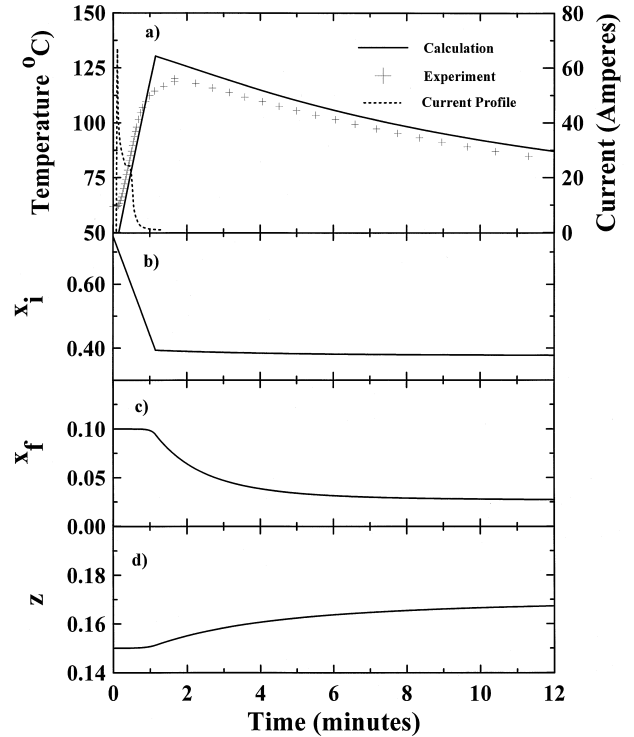


Fig. 10. Measured and calculated short-circuit profiles. The measurement was made on an 18650 cell containing an inert  $\text{LiMn}_2\text{O}_4$  cathode and the calculation is based on a self-heating model for lithiated MCMB in electrolyte. (a) the calculated and measured temperature profiles and the measured current during the experiment; (b) the change in the amount of intercalated lithium; (c) the change in the amount of metastable SEI components; (d) the growth of the reaction product layer. The model used the following values for the parameters in Eq. (6):  $h_1/C = 150x_{f0}$ ,  $A_1 = 1.25 \times 10^{17} \text{ min}^{-1}$ ,  $E_1 = 1.4 \text{ eV}$ ,  $x_{f0} = 0.10$ ,  $n = 0.5$ ,  $h_2/C = 325x_{i0}$ ,  $A_2 = 1 \times 10^8 \text{ min}^{-1}$ ,  $E_2 = 0.8 \text{ eV}$ ,  $x_{i0} = 0.75$  (for a cell discharged to 0.0 V),  $z_0 = 0.15$ .

NEC Moli Energy show that the cell only reached  $120^\circ\text{C}$ . This discrepancy occurs because the calculation predicts the core temperature of the cell whereas the experiment measured the temperature of the cell can.

The assumption that the self-heating in an abused cell occurs because of the reactions at the anode can also be used to predict the behaviour of a cell during an oven exposure experiment.

The oven exposure profiles are calculated by assuming the following.

(1) When  $T_{\text{cell}} < T_{\text{env}}$ , heat will flow into the cell. The rate of heat flow into the cell depends on the cell can and how the cell is prepared for the test (is the label on the can, how is the thermocouple attached).

(2) Heat is generated by the reaction of MCMB. The behaviour of the cathode is ignored so the numerical model from [7] can be used.

The results for a  $150^\circ\text{C}$  oven exposure calculation are shown in Fig. 11. Based on the calculation, a lithium-ion cell containing an MCMB anode and an inert cathode in  $\text{LiPF}_6$  EC:DEC (33:67) overshoots the environmental tem-

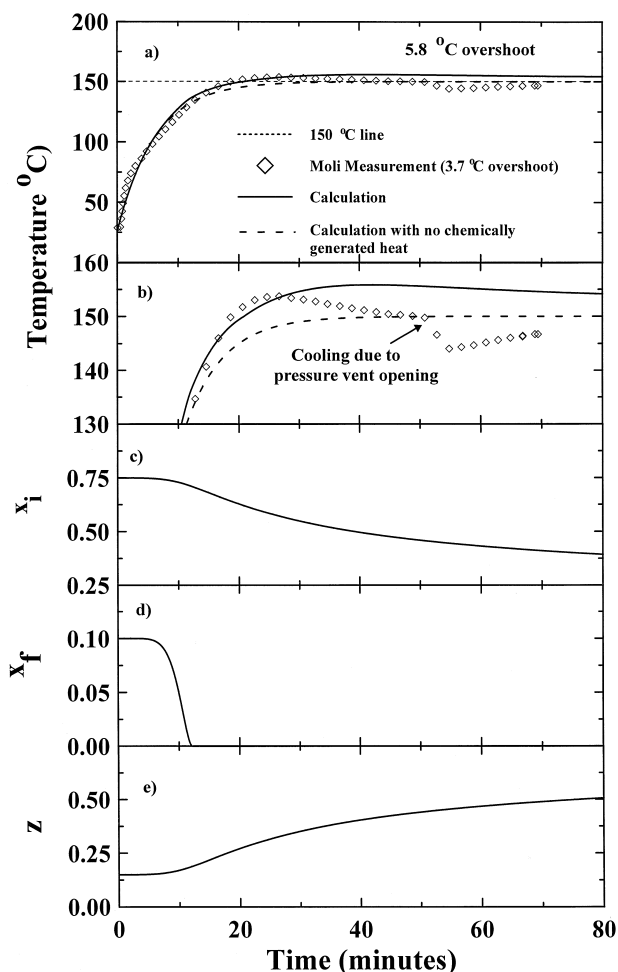


Fig. 11. Calculated and measured oven exposure profiles for an 18650 cell containing a lithiated MCMC anode and an inert  $\text{LiMn}_2\text{O}_4$  cathode. (a) the calculated and measured temperature profiles for an 18650 cell during a  $150^\circ\text{C}$  oven exposure experiment; (b) an expanded view of the measured and calculated temperature overshoots; (c) the change in the amount of intercalated lithium; (d) the change in the amount of metastable SEI components; (e) the growth of the reaction product layer.

perature by about  $5.8^\circ\text{C}$ . The concentration of intercalated lithium,  $x_i$ , and lithium in the metastable SEI,  $x_f$ , start decreasing at approximately  $80^\circ\text{C}$ , hence self-heating starts at this point. The calculated oven exposure profiles agree reasonably well with the experimental oven exposure results obtained from NEC Moli Energy. The NEC Moli Energy cells overshoot the oven temperature by about  $4^\circ\text{C}$ .

We showed in Ref. [2] that the specific composition of the electrolyte affects the self-heating behaviour, so it is surprising that our results agree so well with the NEC Moli Energy results since we do not know which electrolyte is in the NEC Moli cells.

#### 4. Conclusion

ARC experiments have previously been shown to give useful qualitative results concerning the effects of lithium

content, surface area, electrolyte type and initial heating temperature on the reactivity of an electrode material. The results have also been used to determine the kinetic parameters for the conversion of metastable SEI components to stable SEI components. The combination of the qualitative trends and the quantitative kinetic parameters for the reaction(s) allowed us to develop a simple reaction mechanism.

Here we have shown that in addition to being a good tool for a qualitative study, the ARC provides results that can be used to predict the behaviour of practical lithium-ion cells. In particular, ARC results have been used to predict the necessary shutdown temperature for a separator in a cell containing particular electrodes in electrolyte. Similar studies could be done to determine the shutdown temperature necessary for other electrode–electrolyte systems.

The ARC results have also been used, quite successfully, to predict short-circuit and oven exposure profiles for 18650 cells. Our ability to make predictions about the behaviour of practical cells will only improve as we take into account the behaviour of the cathode in electrolyte and the specific composition of the electrolyte itself. Most importantly, the same methods can be used to predict the behaviour of larger cells, such as those for electric vehicles (EV). There is, however, much more work to be done and we encourage others to help out.

#### 5. List of symbols

$A_1$	Frequency factor for the conversion of metastable SEI to stable SEI
$A_2$	Frequency factor for the reaction of intercalated lithium with electrolyte
$C$	Specific heat of the ARC sample
$dT/dt$	Self-heating rate
$E_1$	Activation energy for the conversion of metastable SEI to stable SEI
$E_2$	Activation energy for the reaction of intercalated lithium with electrolyte
$h_1$	Heat of reaction for the formation of stable SEI from metastable SEI
$h_2$	Heat of reaction of intercalated lithium with solvent to eventually form stable SEI
$I$	Current
$k_B$	Boltzmann's constant
$m_{18650}$	Mass of material in an 18650 cell
$m_{\text{ARC}}$	Mass of material in an ARC sample
$n$	Reaction order
$P$	Power
$P_{18650}$	Power generated by the material in an 18650 cell
$P_{\text{ARC}}$	Power generated by the material in an ARC sample
$P_{\text{chem}}$	Chemically generated power, due to chemical reactions
$P_{\text{elec}}$	Electrically generated power, due to short circuit

$P_{\text{out}}$	Power lost to the environment through conduction and convection
$T$	Temperature
$V$	Voltage
$x_f$	Amount of lithium in the metastable SEI
$x_i$	Amount of intercalated lithium
$z$	Amount of lithium in the SEI per unit surface area
$z_0$	Initial amount of lithium in the SEI per unit surface area

### Acknowledgements

The authors thank Ulrich von Sacken of NEC Moli Energy for use of the short-circuit and oven exposure results on IMR18650 cells, and 3M Canada and NSERC

for the support of this work under the Industrial Research Chair program.

### References

- [1] Underwriters Laboratories, Standard for Safety 1642-Lithium Batteries, April, 1995.
- [2] M.N. Richard, J.R. Dahn, *J. Electrochem. Soc.* (1999) in press.
- [3] Y. Xia, M. Yoshio, *J. Electrochem. Soc.* 143 (3) (1996) 825.
- [4] J.-M. Tarascon, W.R. McKinnon, F. Coowar, T.N. Bowner, G. Amatucci, *J. Electrochem. Soc.* 141 (1994) 1421.
- [5] J.N. Reimers, M. Gee, U. von Sacken, *J. Electrochem. Soc.*, submitted May, 1998.
- [6] Y.S. Touloukian, E.H. Buyco, *Thermophysical Properties of Matter—The TPRC Data Series, Vol. 5, Specific Heat—Nonmetallic Solids*, Plenum, New York, 1970.
- [7] M.N. Richard, J.R. Dahn, *J. Electrochem. Soc.* (1999) in press.
- [8] A. Wilson, Moli Energy (1990), private communication, 1998.